SUPPLEMENTARY MATERIALS

Materials and Methods

Testing of DNA oligonucleotides in HEK293 reporter cell lines

A HEK293-based reporter cell line stably expressing human TLR9 and an inducible SEAP (secreted embryonic alkaline phosphatase) reporter gene was obtained (HEK-Blue hTLR9, Invivogen). The SEAP gene is under the control of the IFN-β minimal promoter fused to five NF-kB and AP-1 binding sites. Stimulation with a potent TLR9 ligand such as ODN 2006, which contains 4 CpG sites, activates NF-kB and AP-1, and therefore induces the production of SEAP. SEAP activity can subsequently be measured to quantify the amount of NF-κB response, indicating inflammation. All single-stranded DNA oligonucleotides were synthesized with a phosphorothioate backbone for increased stability (IDT). A list of the DNA sequences used is shown in table S1. ODN 2006 was directly linked to indicated sequence with no intervening nucleotides, or with an AAAAA linker sequence. ODN Control1 (15 nt) and ODN Control2 (24 nt) were selected to match the approximate range of lengths of the various TLR9 inhibitory oligonucleotides and were not expected to inhibit or stimulate TLR9. Indicated concentrations of oligonucleotides (or no oligonucleotides: mock) were incubated with 6 x 10^4 HEK293-TLR9 cells in 200 μl of Dulbecco's Modified Eagle Medium (DMEM) growth media per well in 96-well flat bottom plates for 18 h. 50 ul media was aspirated and incubated with 150 ul HEK-Blue Detection media (Invivogen) for 1 - 6 h at 37°C to allow sufficient color change. Absorbance was then read at 630 nm on a Synergy HT microplate reader (BioTek). Similarly, HEK293 reporter cell lines stably expressing inducible SEAP reporter gene and human TLR7 (1 x 10^5 cells) or TLR2 (6 x 10^4 cells) were stimulated with 1 μg/ml of Gardiquimod or 100 ng/ml of FSL-1 (all reagents from Invivogen) respectively with or without oligonucleotides for 18 h, after which SEAP activity was measured.

For IL-8 production, supernatant was analyzed using an ELISA kit for human IL-8 (BMS204-3INST, Thermo Fisher).

Human PBMCs and intracellular cytokine staining (ICS)

Cryopreserved peripheral blood mononuclear cells (PBMCs) from de-identified healthy donors were purchased from Cellular Technology Limited (CTL). The cryopreserved cells were obtained from commercial providers with written informed consent from the donor and were used in

accordance with Declaration of Helsinki principles. Briefly, the PBMC cryovials stored in liquid nitrogen were thawed for 5 minutes at 37 °C, and the content of each cryovial was transferred to a 15 mL Falcon tube. Tubes were filled with 10 mL AIM-V Glutamax medium (Gibco) containing benzonase (MilliporeSigma). Cells were washed and resuspended at a final concentration of 10^7 cells/mL in AIM-V medium with plasmocin (InvivoGen). For dendritic cell (DC) stimulation, PBMCs were seeded at 5×10^6 cells per well in a 24-well plate, together with the AAV vectors AAV2.GFP.WPRE or AAV2.GFP.WPRE.io2 at 3×10^{10} vg/well. LPS (InvivoGen) was used as positive control at 5 µg/ml. PBMCs from 13 donors were used and cells were incubated for 24 h prior to harvest and staining. Before intracellular and surface staining, cytokine secretion was blocked for 5 h with a mix of Brefeldin A and Monensin (BD Biosciences). Wells were then washed with AIM-V medium to remove non-adherent cells. A cell scraper was used to recover the activated, adherent DCs, which were treated with FcR binding inhibitor (Thermo-Fisher). DC-surface staining was performed with anti-human CD3 (Beckman Coulter), CD19 (Beckman Coulter), CD14 (BD Horizon), CD11c (Thermo-Fisher) and HLA-DR (BD Biosciences). Dead cells were stained with Zombie Yellow Fixable Viability kit (BioLegend). Fixation and permeabilization of cells was performed with Cytofix/Cyto-perm (BD Biosciences). DCs were intracellularly stained with antibodies against human IL-1β (511710, BioLegend) and IL-6 (17-7069, Thermo-Fisher). Fluorescence was measured on a Cytoflex S flow cytometer (Beckman Coulter), and results analyzed with the FlowJo software (Tree Star, Inc.).

For intracellular IFN-β staining, PBMCs from 7 donors were seeded as described and stimulated overnight with vectors AAV2.GFP.WPRE or AAV2.GFP.WPRE.io2 at 5×10^{10} vg/well, or with 5 µg/ml of LPS as positive control. After 5 h incubation with Brefeldin A and Monensin, cells were stained for the surface markers CD3, CD19, CD14, CD11c and HLA-DR, and for viability with Zombie Yellow Fixable Viability kit. After cell fixation and permeabilization, intracellular staining was performed with an anti-human IFNβ antibody (MBS531514, MyBiosource) and signal acquired on a Cytoflex S flow cytometer. Results were analyzed with the FlowJo software.

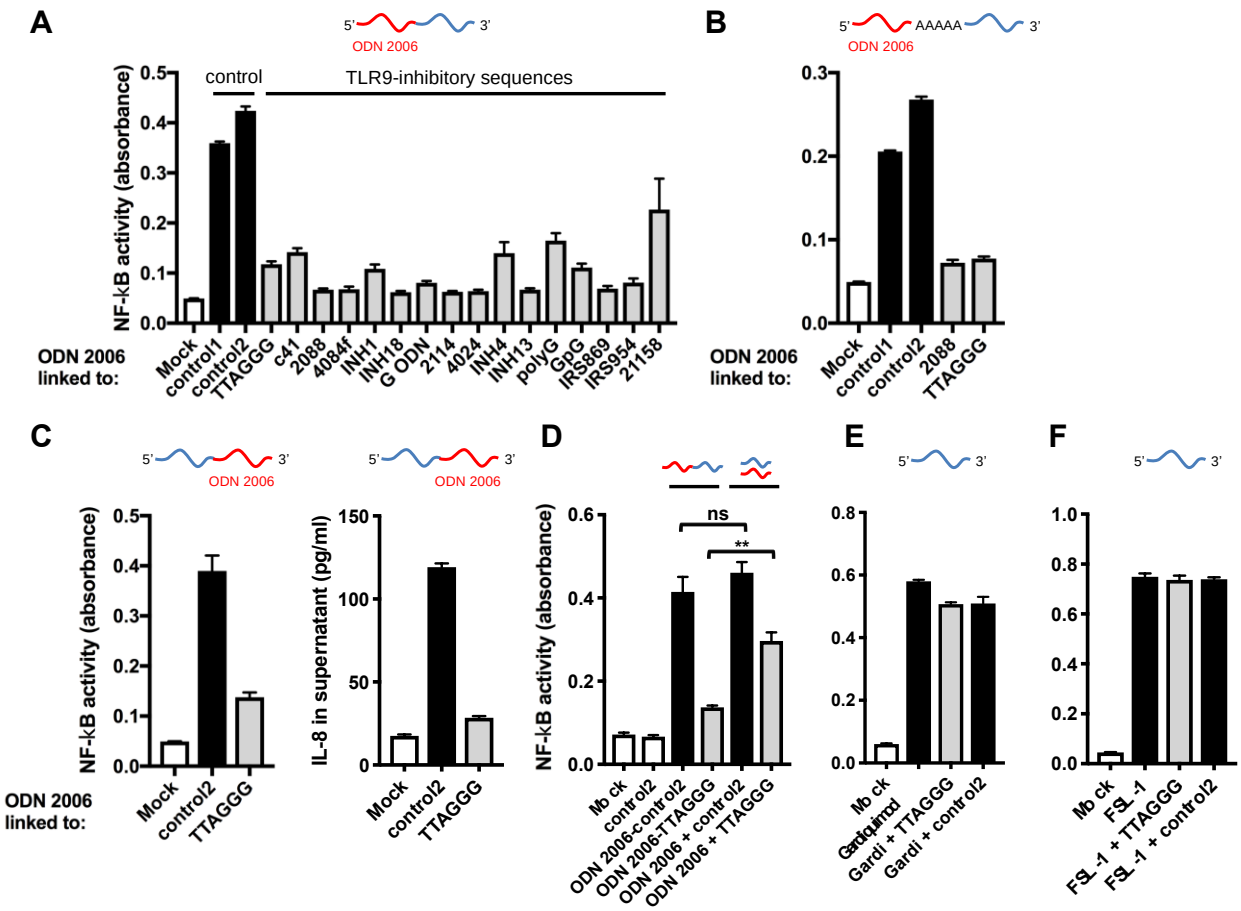

Figure S1. NF-kB response to single-stranded DNA oligonucleotides in reporter cells in vitro.

(**A** and **B**) NF-kB response by HEK293-TLR9 reporter cells after treatment with indicated oligonucleotides at 0.5 μM. Data shown are mean ± s.d. of *n* = 3 biological replicates. (**C**) NF-kB response (left panel) and IL-8 response (right panel) by HEK293-TLR9 reporter cells after treatment with indicated oligonucleotides at 0.5 μM. Data shown are mean ± s.d. of *n* = 3 biological replicates. (**D**) NF-kB response by HEK293-TLR9 reporter cells after treatment with 0.02 μM of linked oligonucleotides or unlinked oligonucleotides (ODN 2006 and other oligonucleotides co-administered as separate molecules, also at 0.02 μM each). Data shown are mean ± s.d. of *n* = 3 biological replicates. ** $p<0.005$ by two-tailed Student's t test. ns, not significant, $p>0.05$. (**E**) NF-kB response by HEK293-TLR7 after treatment with Gardiquimod with or without a high concentration of oligonucleotides at 5 μM. Data shown are mean ± s.d. of *n* = 3 biological replicates. (**F**) NF-kB response by HEK293-TLR2 reporter cells after treatment with FSL-1 with or without a high concentration of oligonucleotides at 5 μM. Data shown are mean ± s.d. of *n* = 3 biological replicates.

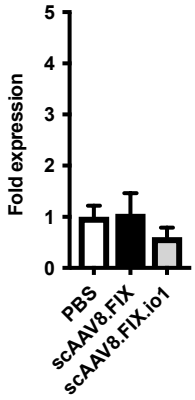

Figure S2. Innate immune response in mice 4 hpi.
Ifnb1 expression in liver assayed by qPCR 4 h after intravenous AAV8 administration (1×10^{11} vg) in C57BL/6 mice. PBS injection was set to 1-fold *Ifnb1* expression. Data shown are mean ± s.e.m. of $n = 5$ animals per condition.

A

Neutralizing antibody titers against AAV8

Condition	Animal #	IC50 NAb for AAV8 (dilution)
PBS	1	<1/40
	2	1/40 to 1/120
	3	1/40 to 1/120
	4	1/40 to 1/120
	5	1/40 to 1/120
scAAV8.FIX	1	1/1080 to 1/3240
	2	1/1080 to 1/3240
	3	1/360 to 1/1080
	4	1/360 to 1/1080
	5	1/120 to 1/360
	6	1/1080 to 1/3240
	7	1/360 to 1/1080
scAAV8.FIX.io1	1	1/360 to 1/1080
	2	1/360 to 1/1080
	3	1/120 to 1/360
	4	1/360 to 1/1080
	5	1/360 to 1/1080
	6	1/360 to 1/1080
	7	1/360 to 1/1080

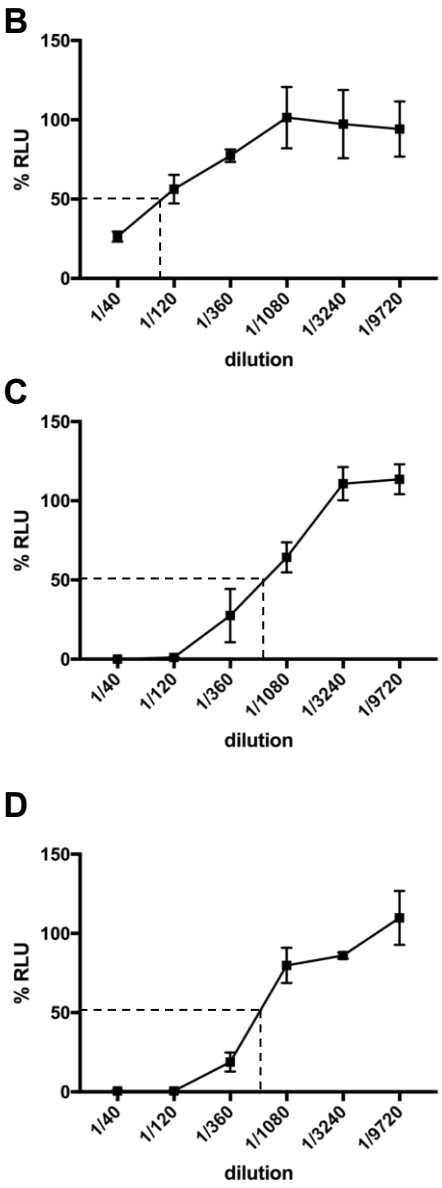

Figure S3. Development of AAV8 neutralizing antibodies (NAb) after vector administration in mice.

Sera from C57BL/6 mice treated with PBS (*n* = 5) or 1 x 10^{11} vg scAAV8.FIX vectors (*n* = 7 each) 28 dpi were tested for neutralizing antibodies against AAV8 using an in vitro Huh7.5 cell assay with an AAV8-β-gal vector. (**A**) Summary of IC50 NAb titers. (**B**) Representative neutralization curve from PBS-treated animals. (**C**) Representative neutralization curve from scAAV8.FIX-treated animals. (**D**) Representative neutralization curve from scAAV8.FIX.io1-treated animals. Dpi, days post-injection; IC50, dilution of serum that inhibits % RLU by 50%; RLU, relative luminometer unit.

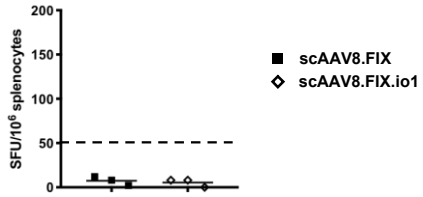

Figure S4. CD8+ T cell responses to AAV8 capsid 21 d after intravenous injections in mice. C57BL/6 mice were injected with 1 x 10^{11} vg scAAV8.FIX or scAAV8.FIX.io1 (n = 3) and an IFN-γ ELISpot assay was performed 21 dpi using an immunodominant peptide. Dotted line (50 SFU/10^6 splenocytes) indicates cutoff for a positive T cell response.

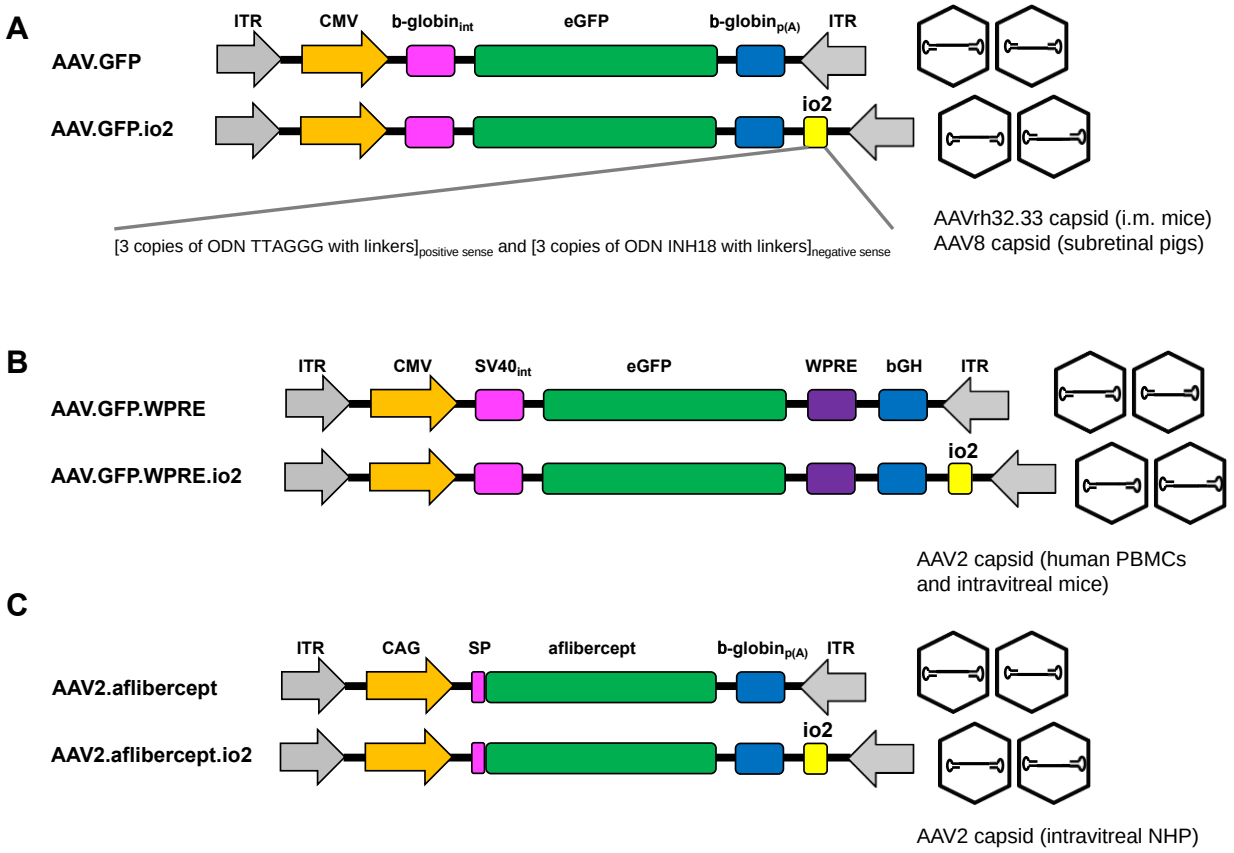

Figure S5. Engineered single-stranded vectors.
(**A**) Schematic diagram of vector organization of AAV.GFP (the original "wild-type" vector) and AAV.GFP.io2 (the "engineered" vector). AAV vectors were packaged in the rh32.33 capsid for intramuscular injections in mice in vivo, and in AAV8 for subretinal injections in pigs in vivo. (**B**) Schematic diagram of vector organization of AAV.GFP.WPRE (the original "wild-type" vector) and AAV.GFP.WPRE.io2 (the "engineered" vector). AAV vectors were packaged in the AAV2 capsid for human PBMCs in vitro. (**C**) Schematic diagram of vector organization of AAV2.aflibercept and AAV2.aflibercept.io2. AAV vectors were packaged into the AAV2 capsid for intravitreal injections in NHPs in vivo. In (**A**), (**B**) and (**C**), the io2 sequence is not expected to be transcribed or translated due to its placement in an untranslated region of the vector downstream of the poly(A) signal. As single-stranded AAV vectors have an equal chance of packaging positive or negative strands of the viral genome, io2 is designed to include both sense and anti-sense TLR9-inhibitory sequences, ensuring that all packaged AAV genomes will carry copies of TLR9-inhibitory sequences in the right orientation. b-globin$_{p(A)}$, beta-globin poly(A) signal; bGH, bovine growth hormone poly(A) signal; CAG, CMV enhancer, chicken β-actin promoter, chimeric intron; CMV, cytomegalovirus promoter; ITR, inverted terminal repeat; SP, human growth hormone signal peptide; SV40$_{int}$, SV40 intron; WPRE, Woodchuck Hepatitis Virus Posttranscriptional Regulatory Element.

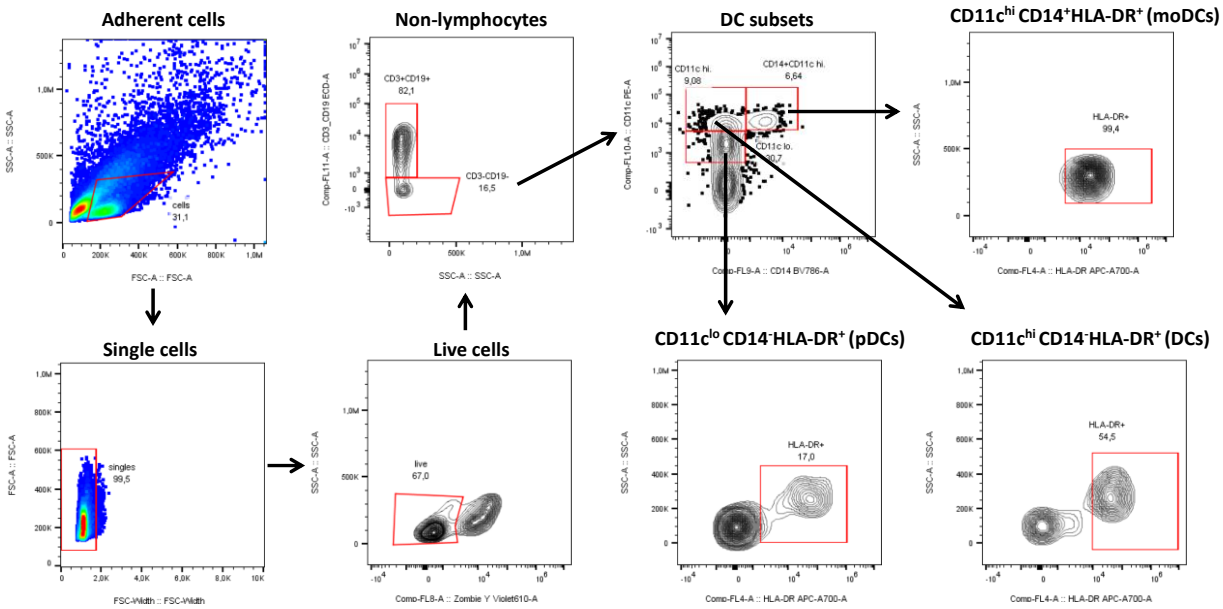

Figure S6. Gating strategy for the different DC subsets.
Adherent cells were harvested 24 hours after incubation of primary human PBMCs with the AAV vectors. Cells were gated on single cells and live cells. After exclusion of CD3+ and CD19+ lymphocytes, cells were gated on DC subsets and positivity for IL-1β and IL-6 was determined in each subset. pDC, plasmacytoid dendritic cell; moDC, monocyte-derived dendritic cell; DC, conventional dendritic cell.

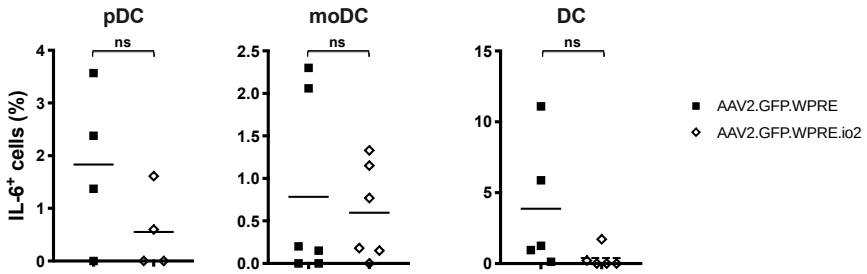

Figure S7. IL-6 immune responses to AAV2 vectors in primary human PBMCs.
Intracellular cytokine staining of IL-6 after infection of primary human PBMCs from 11 donors and analyzing specific DC populations. Some donors did not respond to AAV stimulation and hence are not shown. A two-tailed Wilcoxon matched-pairs signed ranked tested was used. ns, not significant, $p>0.05$. pDC, plasmacytoid dendritic cell; moDC, monocyte-derived dendritic cell; DC, conventional dendritic cell.

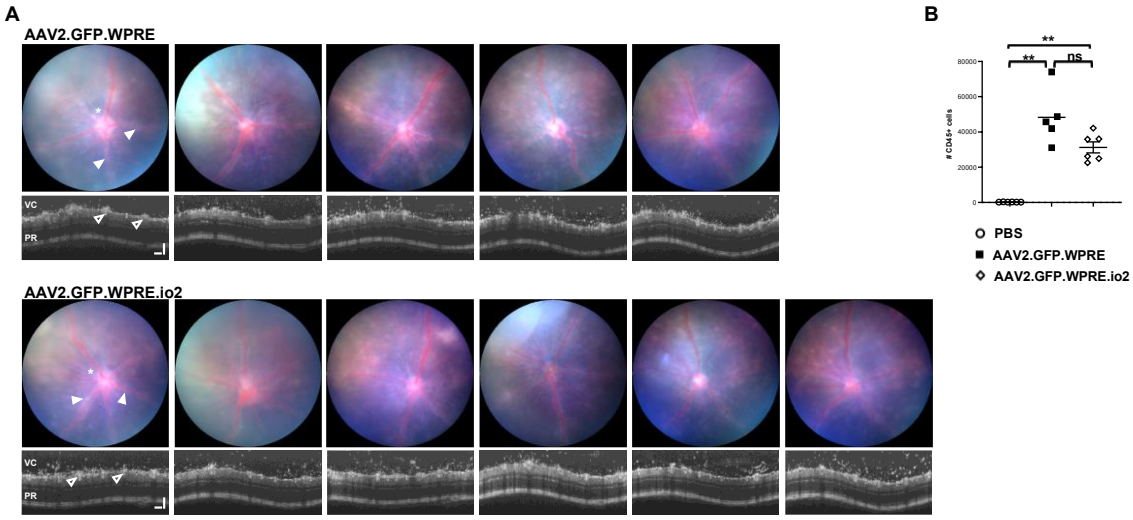

Figure S8. Clinical inflammation in mouse eyes after intravitreal AAV injection.
(A) Fundus and OCT in vivo retinal images captured on day 10 from the AAV2.GFP.WPRE or AAV2.GFP.WPRE.io2 groups demonstrate retinal inflammation. Image annotations: optic disc (*), vasculitis (solid white arrow), vitreous cavity (VC), retinal vessels (open white arrow), photoreceptor layer (PR). By OCT, infiltrating cells entrapped within the optically empty vitreous gel above the retinal tissue are visualized as white dots. (**B**) At day 11 post-injection, eyes were dissected and processed by flow cytometry to identify and enumerate the absolute number of CD45+ cells. *n* = 5-6 eyes per group as indicated. ns, not significant $p>0.05$, **$p<0.005$ by two-tailed Mann-Whitney test.

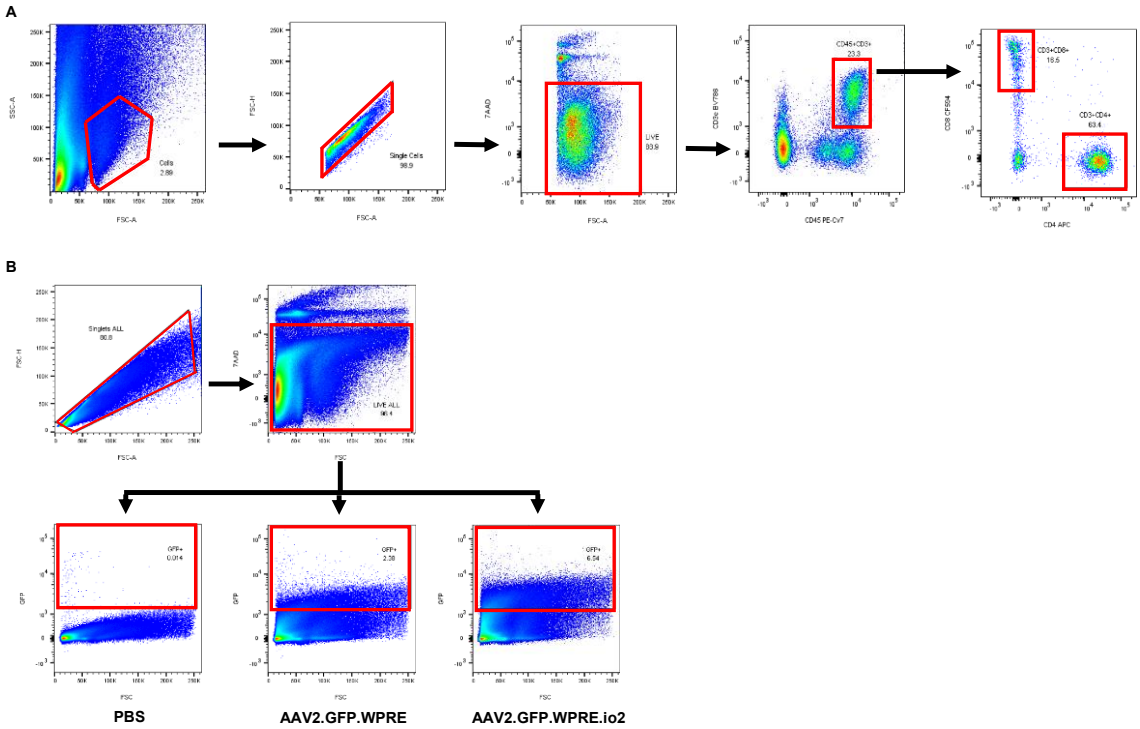

Figure S9. Flow cytometry gating strategy for ocular infiltrating immune cell populations and GFP+ retinal cells from mice.

(**A**) Individual retinas were dissected and processed for flow cytometry at day 11 post intravitreal injection with AAV vectors or PBS control. Retinas were gated for scatter profiles, singlets, live cells, and CD45+CD3+ subsets (CD4+ vs CD8+). (**B**) To determine differences in AAV expression from these samples, retinal cells were gated for singlets, live cells and GFP+ expression by geometric MFI or GFP fluorescence above a uniformly applied threshold.

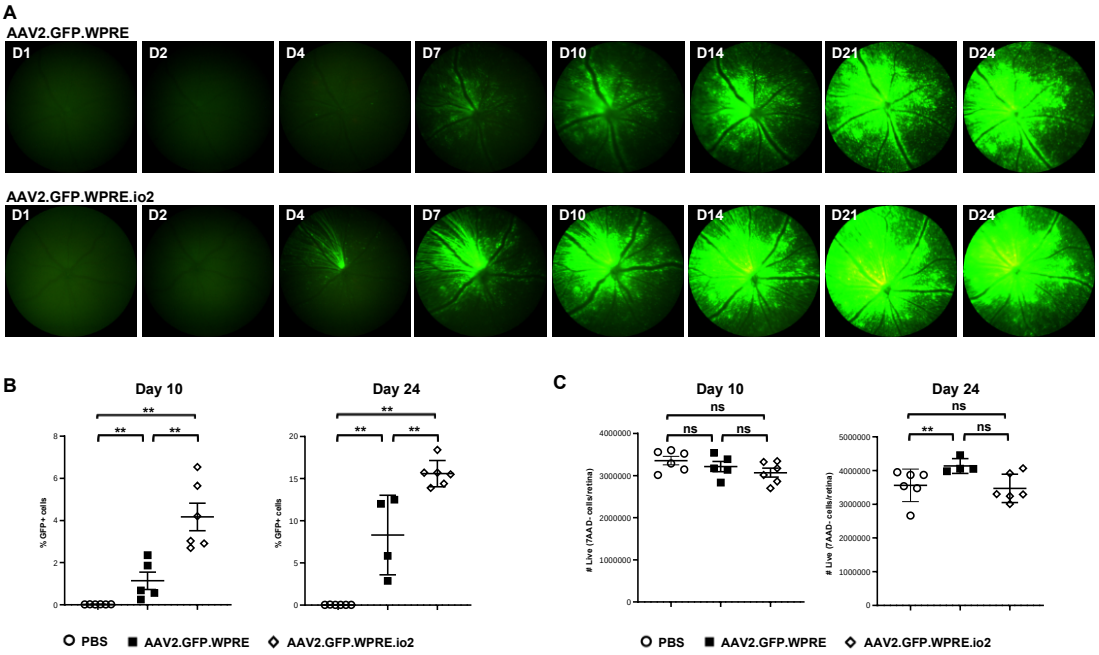

Figure S10. Time course of GFP expression and viability after intravitreal AAV injection in mice.

(**A**) Clinical time course demonstrating GFP expression in representative single mouse eyes injected with either AAV2.GFP.WPRE or AAV2.GFP.WPRE.io2. (**B**) Flow cytometric analysis indicates percentage (%) of GFP+ cells in the retinas from mice culled at day 10 and day 24 post-injection of AAV2 or PBS. (**C**) The absolute number of viable cells per retina at each time point was calculated based on live cell gate (7AAD- cells). Data shown are mean ± s.d., with each symbol representing one eye. *n* = 4-6 eyes per group as indicated. ns, not significant $p>0.05$, *$p<0.05$ and **$p<0.005$ by two-tailed Mann-Whitney test.

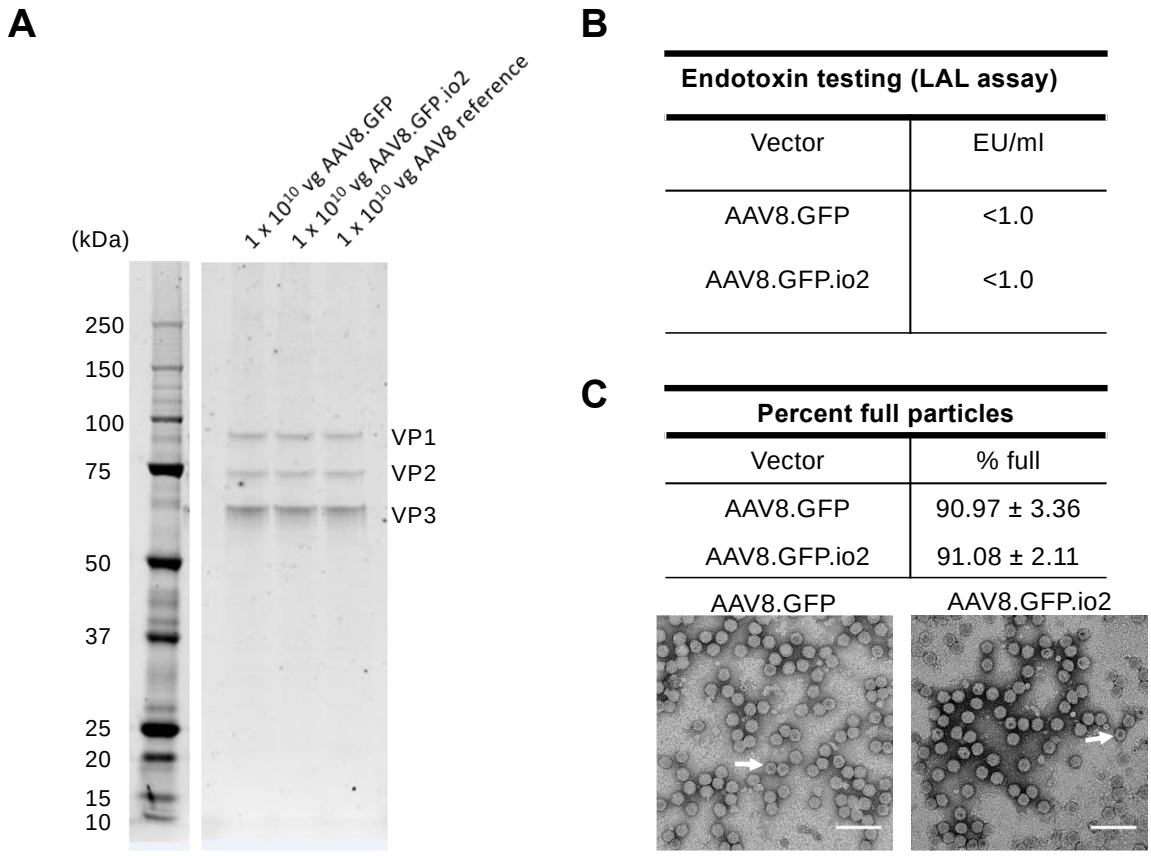

Figure S11. Characterization of AAV8 vectors used in pig study.
(**A**) 1 x 10^{10} vg AAV8 vectors were run on SDS-PAGE followed by silver staining. A protein marker was used to determine approximate sizes of viral proteins (VP). A different AAV8 reference vector from the vector core also was loaded for comparison. (**B**) Endotoxin testing of AAV8 vectors using a limulus amebocyte lysate assay showed that both vectors were endotoxin free (<1 EU/ml). (**C**) Percentage of full particles was determined by negatively staining AAV with 0.5% uranyl acetate and viewing under a transmission electron microscope. Empty particles show an electron-dense circle in the middle of the capsid (example shown with arrow). The number of empty and full particles was counted directly from electron micrographs of ten random images for each vector. 1,183 particles were counted for AAV8.GFP and 1,221 particles were counted for AAV8.GFP.io2. The average percent full particles per image is reported with standard deviation. Representative images are shown for each vector. Scale bar: 100 nm.

Figure S12. Engineered vector evades photoreceptor pathology in subretinal-injected pig eyes.

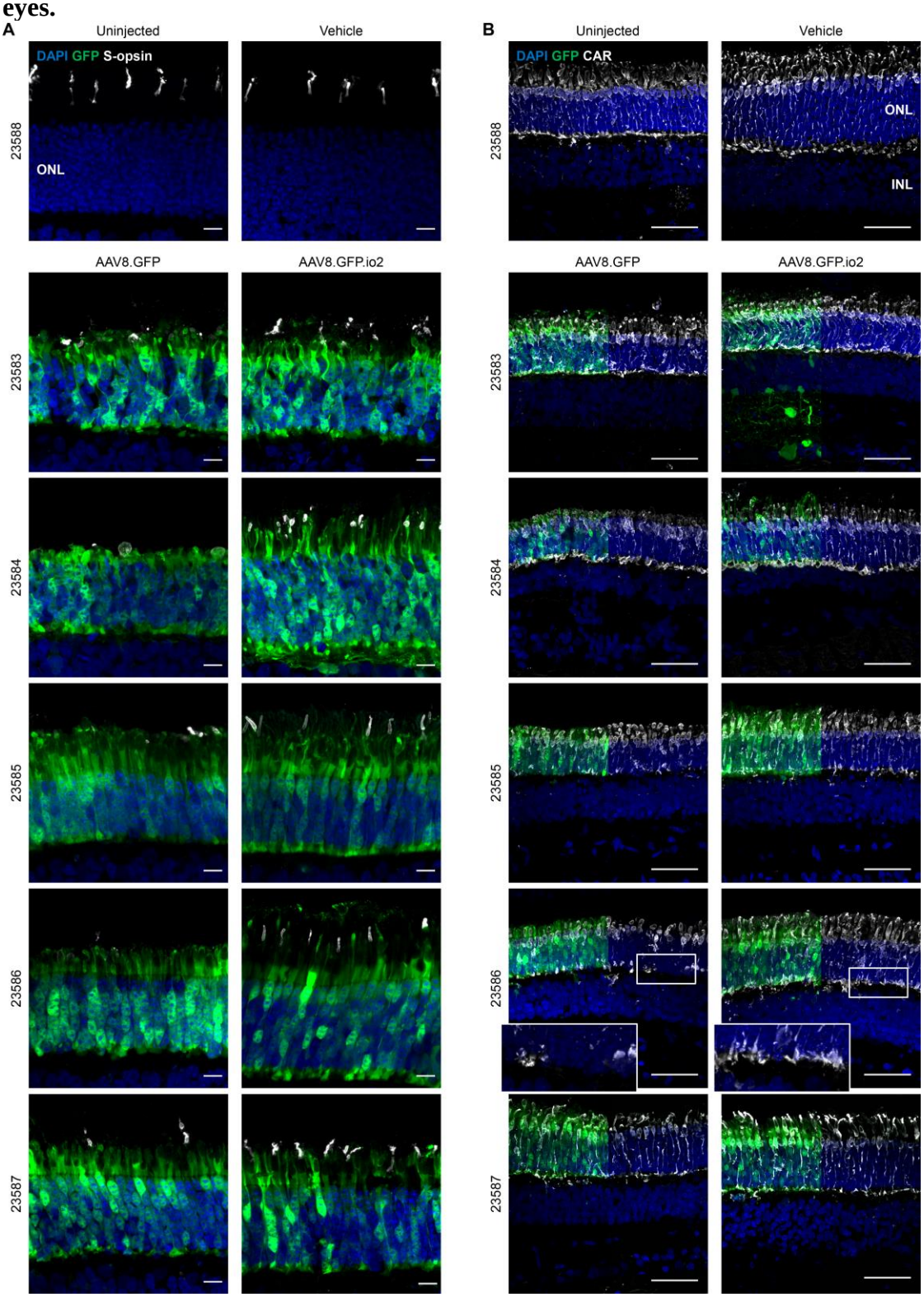

Figure S12. Engineered vector evades photoreceptor pathology in subretinal-injected pig eyes.
Immunohistochemical images of pig retinas 6 weeks after subretinal injections. Each animal is indicated by an identification number and paired images are from the two treated eyes of each animal. (**A**) Outer segments of cone photoreceptors visualized by anti-blue (S) opsin staining. Scale bars, 10 μm. (**B**) Cone photoreceptors visualized by anti-human cone arrestin staining. Scale bars, 50 μm. Regions shown for AAV8-injected eyes are GFP+, but GFP signal from the right half of each image was digitally removed to allow better visualization of arrestin staining. ONL, outer nuclear layer; CAR, cone arrestin.

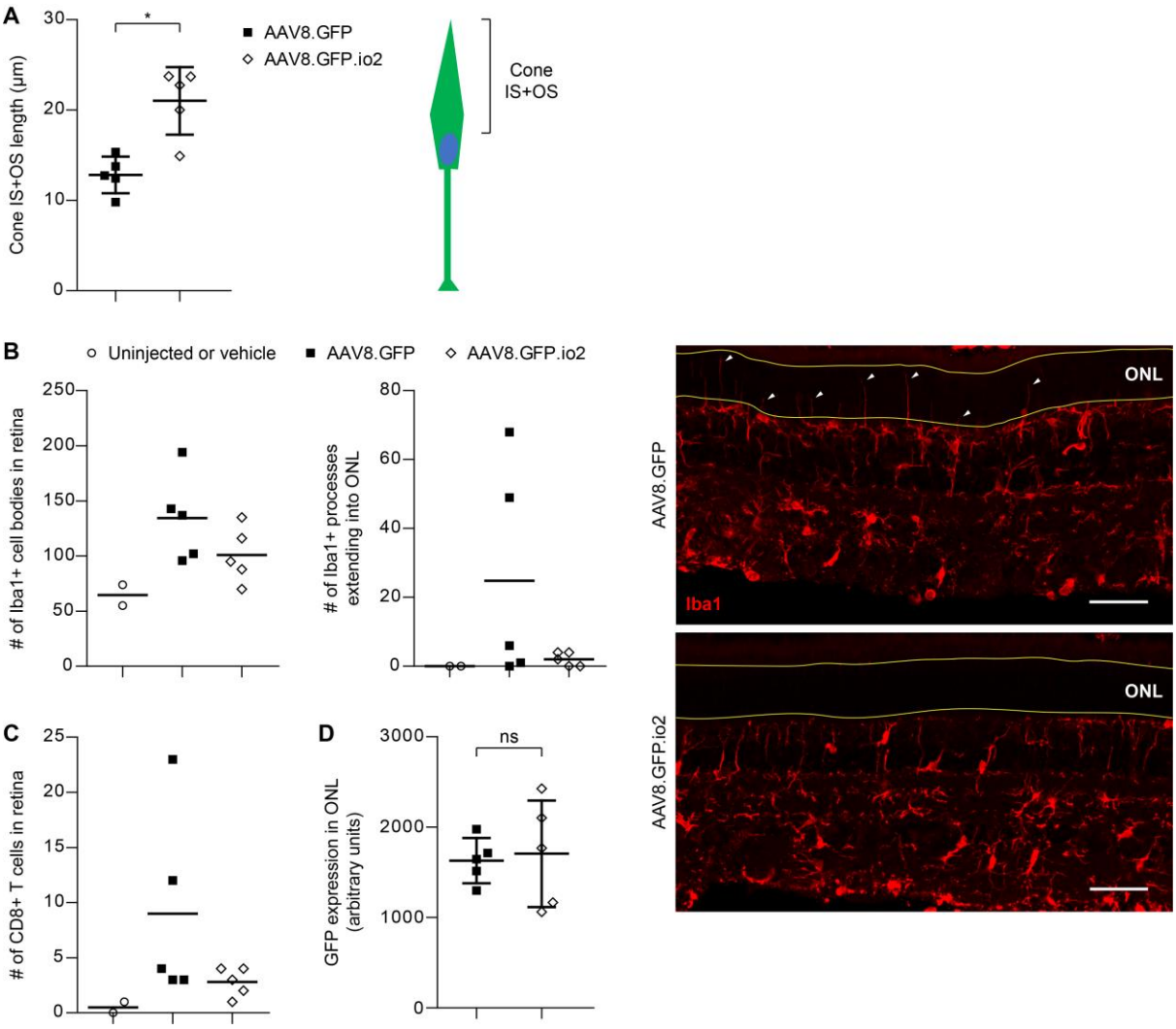

Figure S13. Quantification of retinal pathology in subretinal-injected pig eyes.
(**A**) Quantification of inner segment plus outer segment (IS+OS) length of GFP+ cones, defined as the distance from the apex of the cone outer segment to the proximal edge of the nucleus. For each eye, the mean IS+OS length was calculated from 30 GFP+ cones over at least three separate 20 µm sections. *p<0.05 by two-tailed Mann-Whitney test. (**B**) Quantification of Iba1+ cell bodies in the retina and Iba1+ processes extending into the ONL. For AAV-injected eyes, images of three GFP+ fields of view (20X) from separate 20 µm sections were acquired using a widefield fluorescence microscope and the number of Iba1+ cell bodies in the retina or Iba1+ processes extending into the ONL was counted. For uninjected and vehicle control eyes, three random fields were selected. Example images highlighting Iba1+ processes (white arrows) in the ONL (yellow lines) from animal 23586 are shown. Scale bars, 50 µm. (**C**) Quantification of CD8+ cells in the retina. For AAV-injected eyes, CD8+ cells were counted in ten separate GFP+ fields of view (20X) from at least three separate 20 µm sections. For uninjected and vehicle control eyes, ten random fields were selected. Only CD8+ cells in the retina were counted (RPE, choroid and sclera were excluded from analysis). (**D**) Quantification of GFP signal in the ONL was performed using ImageJ. For each eye, two GFP+ sections were imaged and intensity values were obtained and averaged from the field of view (20X) with the highest GFP signal in each

section. Sections from corresponding OD and OS eyes were imaged under identical conditions. ns, not significant by two-tailed Mann-Whitney test. ONL, outer nuclear layer; Iba1, ionized calcium-binding adaptor protein 1.

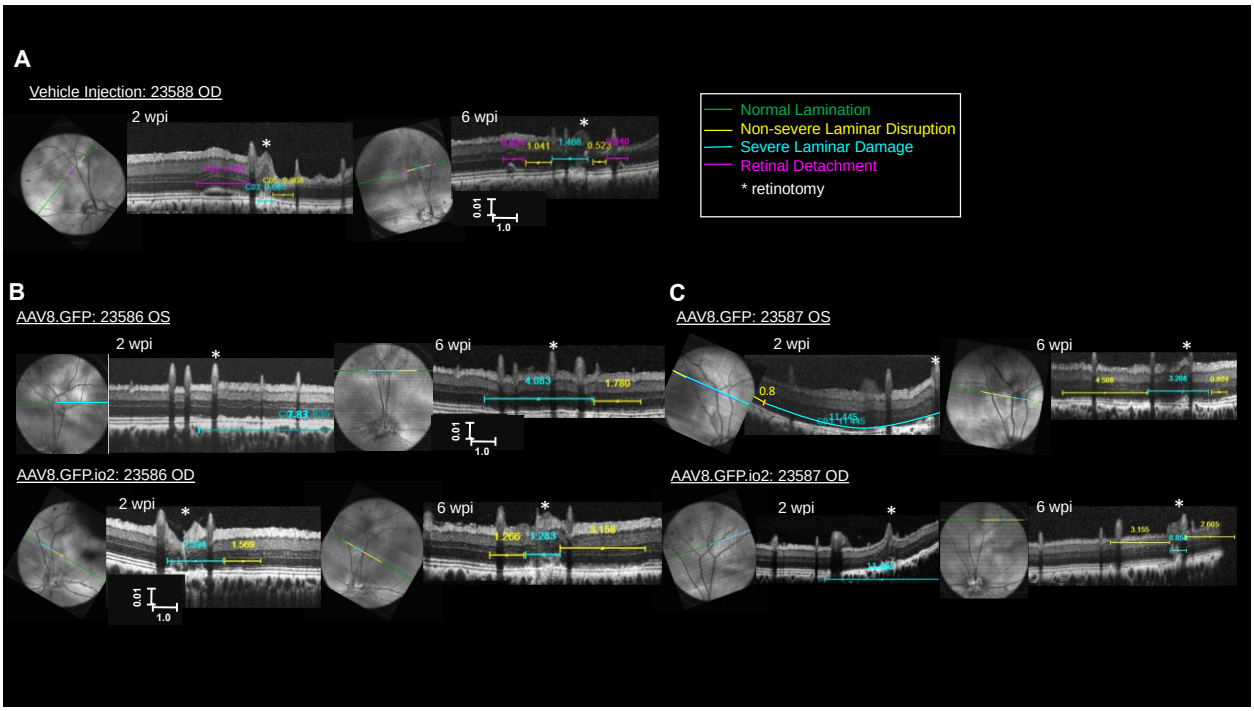

Figure S14. Outer retinal laminar pathology in pigs measured by OCT is consistent with retinal histology.

Representative OCT b-scans in a vehicle-treated eye (**A**) and from two different pigs (**B** and **C**) whose left eye was injected with AAV8.GFP (OS, top) and whose right eye was injected with AAV8.GFP.io2 (OD, bottom). In areas without damage, the outermost hyper-reflective band (located at the bottom of each b-scan) represents the choroid/sclera. Moving inward, the next hyper-reflective band represents the RPE and the third band the IS/OS of the photoreceptors. Different colored calipers indicate areas with differential damage. Severe damage (cyan calipers) were areas where both the photoreceptor and RPE layers were disrupted, non-severe disruption (yellow calipers) were areas where the hyper-reflective bands for one or both of these layers were thinner and less well defined. Retinal detachment was denoted by magenta caliper. Severe damage always surrounded the retinotomy (asterisk) and non-severe disruption always surrounded areas of severe damage. Areas outside of the calipers have normal retinal lamination. The numbers above the horizontal calipers indicates the length of damage (mm). Scale bars also are shown on each b-scan. The fundus image indicates the location of each b-scan on the retina. Images at 2 (left) and 6 wpi (right) are shown for each eye to illustrate whether damage changed with time after injection. Only animals 23586 and 23587 were analyzed as b-scans were available for most of the GFP+ region (mean = 30 mm^2) for both eyes. Animal 23583 was excluded as the area of GFP+ region was unusually small (1.4 mm^2 in each eye) and there was concern that the entire inoculum volume had not been deposited subretinally. Optical coherence tomography, OCT; retinal pigment epithelium, RPE; IS/OS, inner segment/outer segment; wpi, weeks post injection.

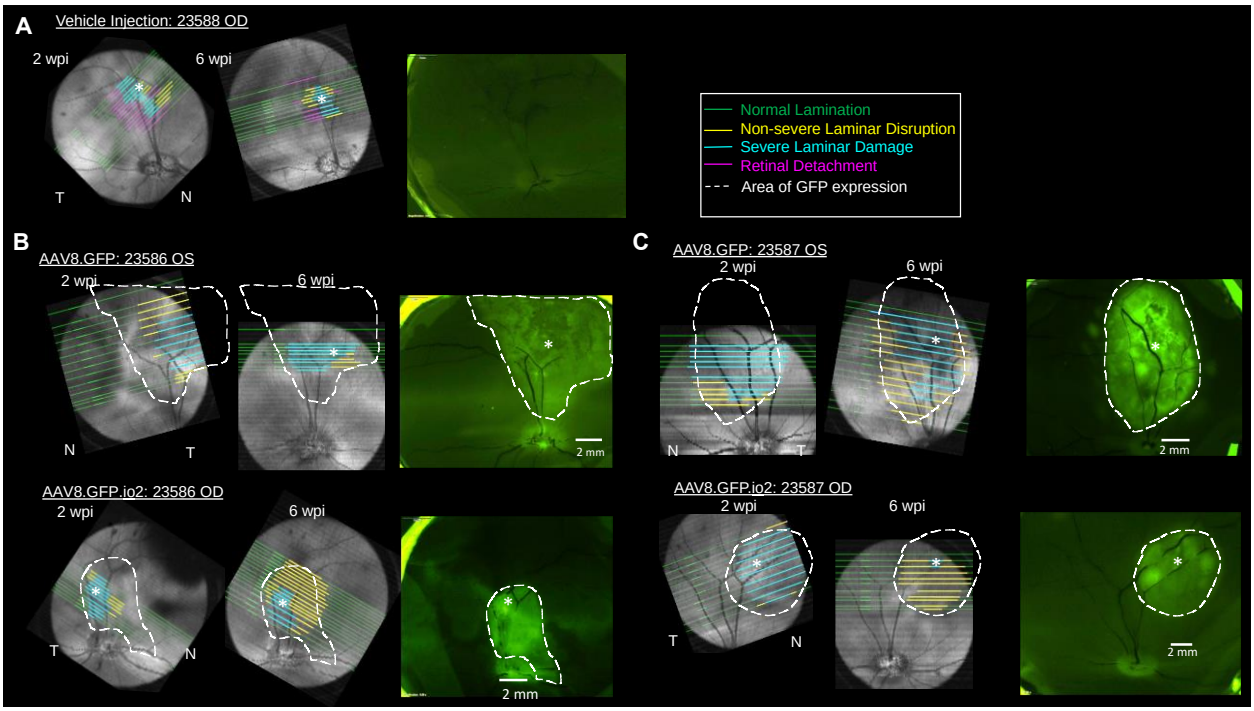

Figure S15. Engineered vector ameliorates outer retina laminar pathology in subretinal-injected pig eyes.

Summary data for the extent of each type of damage are shown on fundus images for eyes injected subretinally with vehicle (**A**) or two pigs (**B** and **C**) whose left eye was injected with AAV8.GFP (OS, top) and whose right eye was injected with AAV8.GFP.io2 (OD, bottom). Superimposed on each fundus image are the retinotomy site (*) and areas of severe damage (cyan) and non-severe disruption (yellow) that were determined from OCT b-scans at 2 and at 6 wpi. Retinal areas with normal outer retina lamination are indicated in green. Severe damage always surrounded the retinotomy (*) and was defined as loss of the hyper-reflective outer retinal bands that represent the RPE and photoreceptor inner/outer segments. Non-severe disruption (yellow) was usually found surrounding areas of severe damage and was defined as areas where the outer retinal hyper-reflective bands were thinner and/or more poorly defined. The fluorescence images of each eye cup are shown (right) and the GFP+ boundary indicated by the dashed white line. As a meaningful statistical analysis could not be performed with the small number of eyes in the study, the results are presented as qualitative observations.

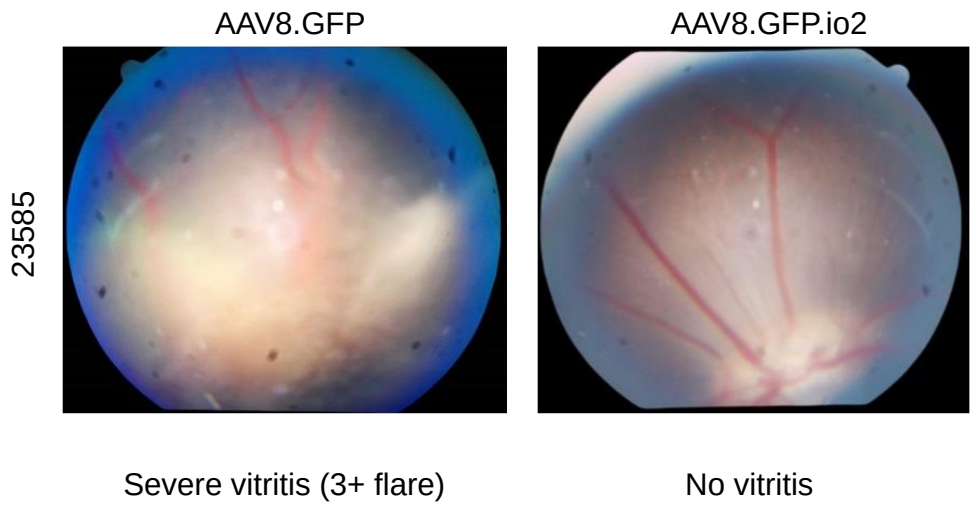

Figure S16. Vitritis in pig 23585.
Fundus images of pig 23585 at 2 wpi. The animal experienced severe vitritis in AAV8.GFP-treated eye, but not AAV8.GFP.io2-treated eye. Vitritis resolved at 6 wpi.

A

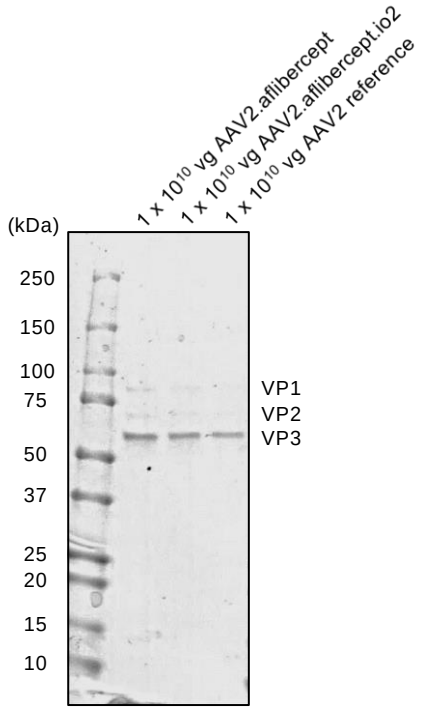

B

Endotoxin testing (LAL assay)

Vector	EU/ml
AAV2.aflibercept	0.1
AAV2.aflibercept.io2	0.07

C

Percent full particles

Vector	% full
AAV2.aflibercept	99.42 ± 0.14
AAV2.aflibercept.io2	99.55 ± 0.41

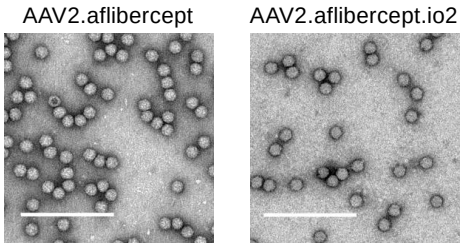

D

Sterility testing

Vector	Medium	Result
AAV2.aflibercept	SCD	No growth
	FTM	No growth
	LB agar	No growth
AAV2.aflibercept.io2	SCD	No growth
	FTM	No growth
	LB agar	No growth
Vehicle	SCD	No growth
	FTM	No growth
	LB agar	No growth

E

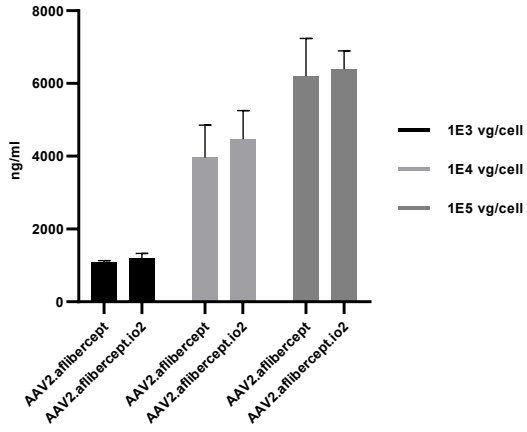

Figure S17. Characterization of AAV2 vectors used in NHP study.
(**A**) 1 x 10^{10} vg AAV2 vectors were run on SDS-PAGE followed by Coomassie staining. A protein marker was used to determine approximate sizes of viral proteins (VP). A different AAV2 reference vector from the vector core also was loaded for comparison. (**B**) Endotoxin testing of AAV2 vectors using a limulus amebocyte lysate assay showed that both vectors were endotoxin free (≤0.1 EU/ml). (**C**) Percentage of full capsids was determined by staining with 1% uranyl acetate and viewing under a transmission electron microscope. The number of full and

empty particles was counted directly from 6 images of each vector. A total of 3,130 particles were counted for AAV2.aflibercept, and 1,106 particles were counted for AAV2.aflibercept.io2. The average percent full particles per image is presented with standard deviation. Representative images are show for each vector. Scale bar: 200 nm. (**D**) Inoculation of the AAV2 vectors and vehicle in microbial growth media confirmed that all preparations were sterile (no growth). (**E**) HeLa cells were transduced with the AAV2 vectors at indicated multiplicity of infections for 48 h and supernatants were analyzed for aflibercept concentration. SCD, soybean casein digest; FTM, fluid thiolglycollate medium; LB, luria broth.

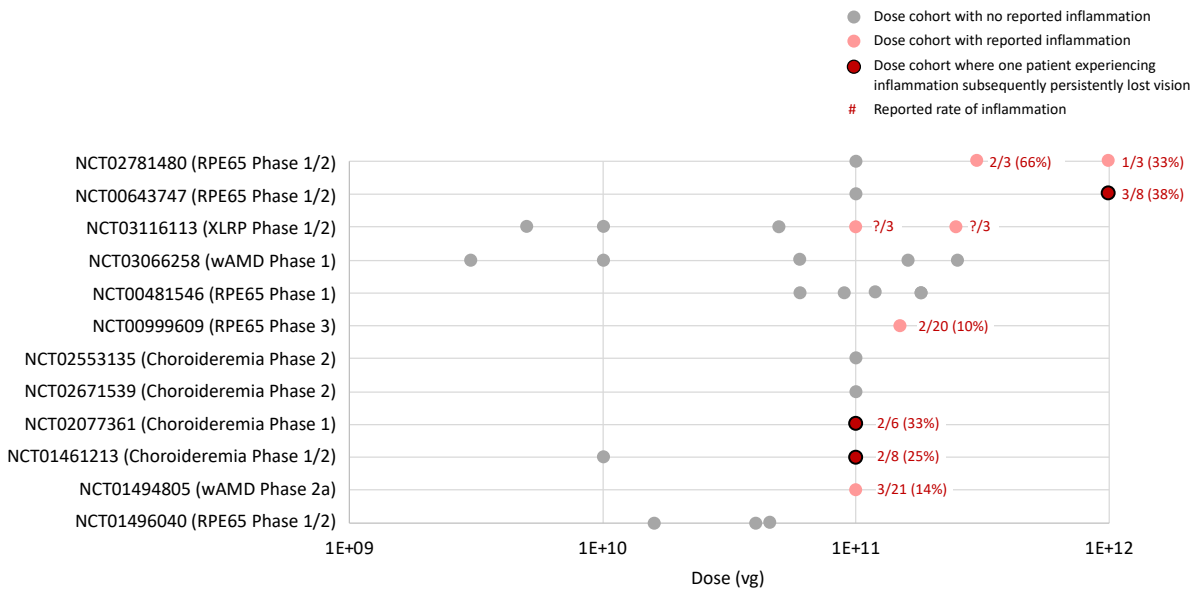

Note: reflects publicly available information as of Nov 30, 2019. Excludes cases of inflammation specified as peri-operative only. Use of prophylactic immunosuppression was reported for vast majority of trials

Figure S18. Ocular inflammation observed in subretinal AAV clinical trials.
Analysis of publicly available information on ocular inflammation in subretinal AAV gene therapy clinical trials. Inflammation occurred in an AAV-dose dependent manner, with reported cases beginning at 1E+11 vg. Capsids used include AAV2, AAV4, AAV5 and AAV8. In each of three separate clinical trials, one patient exhibited persistent loss of some vision following inflammation, which was not observed in the control eye. Most of these clinical trials reported use of prophylactic systemic immunosuppression in the form of oral corticosteroids. XLRP, X-linked retinitis pigmentosa. wAMD, wet age-related macular degeneration.

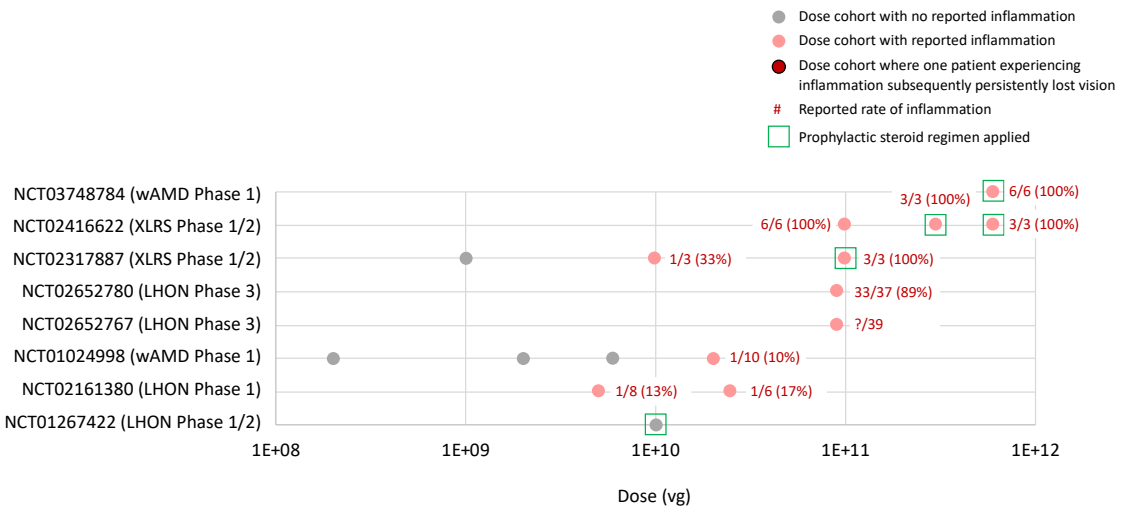

Note: reflects publicly available information as of Nov 30, 2019. Excludes cases of inflammation specified as peri-operative only. Unless otherwise indicated, patients were not prophylactically immunosuppressed

Figure S19. Ocular inflammation observed in intravitreal AAV clinical trials.
Analysis of publicly available information on ocular inflammation in intravitreal AAV gene therapy clinical trials. Inflammation occurred in an AAV-dose dependent manner, with reported cases beginning at 1E+10 vg, which is ten times lower than that for subretinal AAV clinical trials. At doses > 1E+11 vg, ocular inflammation occurred in nearly all patients, despite prophylactic immunosuppression. Capsids used include AAV2 and AAV2 variants (AAV2tYF and AAV2.7m8). Unless indicated otherwise, patients were not prophylactically immunosuppressed. XLRS, X-linked retinoschisis. LHON, Leber's hereditary optic neuropathy. wAMD, wet age-related macular degeneration.

Table S1. Oligonucleotide sequences used in this study.

All oligonucleotides (except io1 and io2, which were part of the AAV vector genome) were synthesized as single-stranded DNA oligonucleotides with a phosphorothiorate backbone for increased stability.

Table S1. Oligonucleotides sequences used in this study			
Name of ODN (reference #)	Sequence (5’ to 3’)	Length (nt)	Comments
2006 (*22, 47*)	TCGTCGTTTTGTCGTTTTGTCGTT	24	
Control1	TCCTGAGCTTGAAGT	15	
Control2	TTATTATTATTATTATTATTATTA	24	
TTAGGG (*23*)	TTAGGGTTAGGGTTAGGGTTAGGG	24	From telomeres
c41 (*48*)	TGGCGCGCACCCACGGCCTG	20	
2088 (*49, 50*)	TCCTGGCGGGGAAGT	15	
4084f (*51*)	CCTGGATGGGAA	12	
INH1 (*51*)	CCTGGATGGGAATTCCCATCCAGG	24	
INH18 (*51*)	CCTGGATGGGAACTTACCGCTGCA	24	
G ODN (*52*)	CTCCTATTGGGGGTTTCCTAT	21	
2114 (*53*)	TCCTGGAGGGGAAGT	15	
4024 (*54*)	TCCTGGATGGGAAGT	15	
INH4 (*51*)	TTCCCATCCAGGCCTGGATGGGAA	24	
INH13 (*51*)	CTTACCGCTGCACCTGGATGGGAA	24	
polyG (*55*)	GGGGGGGGGGGGGGGGGGGG	20	
GpG (*56*)	TGACTGTGAAGGTTAGAGATGA	22	
IRS869 (*57*)	TCCTGGAGGGGTTGT	15	
IRS954 (*57*)	TGCTCCTGGAGGGGTTGT	18	
21158 (*58*)	CCTGGCGGGG	10	
io1 (this study)	TTTAGGGTTAGGGTTAGGGTTAGGGAAAAA TTTAGGGTTAGGGTTAGGGTTAGGGAAAAA TTTAGGGTTAGGGTTAGGGTTAGGGAAAAA	90	For scAAV vectors
io2 (this study)	TTTAGGGTTAGGGTTAGGGTTAGGGAAAAA TTTAGGGTTAGGGTTAGGGTTAGGGAAAAA TTTAGGGTTAGGGTTAGGGTTAGGGAAAAA TGCAGCGGTAAGTTCCCATCCAGGTTTTT TGCAGCGGTAAGTTCCCATCCAGGTTTTT TGCAGCGGTAAGTTCCCATCCAGGTTTTT	177	For ssAAV vectors

Table S2. Study design to evaluate subretinal delivery of AAV vectors in wild-type pigs. Six wild-type female pigs were injected subretinally with 75 µl of indicated AAV8 vectors (4 x 10^{11} vg) or with vehicle control. The animals received clinical examinations at weekly intervals and OCT imaging at 2 wpi and 6 wpi, and were euthanized 6 wpi. N.A., not applicable; OD, oculus dextrus (right eye); OS, oculus sinister (left eye); vg, vector genomes; wpi, weeks post-injection.

Table S2. Study Design to evaluate subretinal delivery of AAV vectors in wild-type pigs.

Animal ID number	Dose (vg)/eye	OD	OS
23583	4 x 10^{11}	AAV8.GFP.io2	AAV8.GFP
23584	4 x 10^{11}	AAV8.GFP.io2	AAV8.GFP
23585	4 x 10^{11}	AAV8.GFP.io2	AAV8.GFP
23586	4 x 10^{11}	AAV8.GFP.io2	AAV8.GFP
23587	4 x 10^{11}	AAV8.GFP.io2	AAV8.GFP
23588	N.A.	Vehicle	Uninjected

Table S3. Summary of findings in pig study, including histology and clinical examinations (inflammation scores).
Immunohistochemical staining in the retina was performed 6 wpi at the terminus of the study. Uveitis via the SUN classification was followed at weekly intervals from 2 wpi to 6 wpi. OCT imaging was performed at baseline (day of injection), 2 wpi and 6 wpi and area of damage to photoreceptor layers are shown for 6 wpi (terminus).

Table S3. Summary of findings in pig study, including histology and clinical examinations (inflammation scores).

Animal ID number	Dose (vg)/eye	Visible loss of cone outer segments	Microglia infiltration	Cytotoxic T cell infiltration	Clinical uveitis
23583	AAV8.GFP	Yes	No	No	No
	AAV8.GFP.io2	No	No	No	No
23584	AAV8.GFP	Yes	No	No	No
	AAV8.GFP.io2	No	No	No	No
23585	AAV8.GFP	Yes*	Yes	Yes	Yes**
	AAV8.GFP.io2	No	No	No	No
23586	AAV8.GFP	Yes*	Yes	Yes	No
	AAV8.GFP.io2	No	No	No	No
23587	AAV8.GFP	Yes	No	No	No
	AAV8.GFP.io2	No	No	No	No
23588	Uninjected	N.A.	No	No	No
	Vehicle	N.A.	No	No	No

*Apparent loss or retraction of cone pedicles observed as well.
**3+ flare at 2 wpi, 1+ flare at 3 wpi, 0.5 flare at 4 wpi, traces of vitritis at 5 wpi, and vitritis resolved at 6 wpi. No steroid treatment was used throughout the course of vitritis. N.A., not applicable; OCT, optical coherence tomography; SUN, Standardization of Uveitis Nomenclature; wpi, week post-injection.

Data File S1. Raw data